Model Predictive Control for a Grid-interactive Efficient Thermal Storage-integrated Heat Pump System

Liang SHI[1], Ming QU[1]*, Xiaobing LIU[2], Jin DONG[2], Borui CUI[2], Lingshi WANG[2]

[1]Purdue University, Lyles School of Civil Engineering,
West Lafayette, IN, USA
shi448@purdue.edu
mqu@purdue.edu

[2]Oak Ridge National Laboratory,
Oak Ridge, TN, USA
liux2@ornl.gov
dongj@ornl.gov
cuib@ornl.gov
wangl2@ornl.gov

* Corresponding Author

ABSTRACT

Building heating and cooling systems can be used to overcome the mismatch between the intermittent supply of renewable power and the fluctuating demand for electricity. A novel underground thermal energy storage integrated with a dual-source heat pump has been proposed to mitigate the mismatch while meeting the thermal demand of buildings efficiently. Conventional thermostat control with heuristic rules cannot provide intelligent decisions to maximize the thermal efficiency and flexibility of the proposed system. Advanced control strategies like model predictive control (MPC) have provided a new paradigm for grid-interactive efficient building operation with the advancement of computation and sensing. This study developed an MPC for the proposed system to provide grid service for Demand Side Management and minimize the operating cost of building owners. A control-oriented dynamic model of the proposed system has been developed. Given an objective function and proper constraints, an optimization problem is formulated to determine the optimal control strategy of the system. Dynamic Programming is adopted to solve the optimization problem. A rule-based control (RBC) is also developed to achieve similar goals. Short-term simulations are conducted to compare the system performance resulting from the two controls. The simulation results indicate that the MPC performs more intelligently than the RBC in charging thermal energy storage and selecting heat pump sources by taking advantage of the predicted cooling demands of the building and the performance of the integrated system. As a result, the MPC could save energy and reduce operating costs compared with the RBC. A case study shows that, for a 3-day operation, the MPC saves 36.9% energy and reduces 38.5% operating cost compared with the RBC.

1. INTRODUCTION

The increasing penetration of intermittent renewable power raises challenges to the existing electric grids due to a mismatch between the supply and demand sides. Buildings consume 74% of all U.S. electricity, and space heating/cooling accounts for 34% and 27% of the electricity consumed in residential and commercial buildings (Schwartz et al., 2017). In addition, space heating/cooling contributes to 46% peak demand of the electric grid (Neukomm et al., 2019). Therefore, large-scale implementation of highly efficient building thermal systems with greater flexibility is a solution to mitigate the mismatch between the intermittent renewable power supply and the fluctuating electric demand in buildings. While thermal energy systems (TES) have been successfully implemented in large commercial buildings for shifting the electricity demand from the on-peak hours to the off-peak hours of the grid, few technologies have been developed for residential buildings to effectively shift electric demand without compromising the thermal comfort of buildings' occupants.

A novel thermal energy storage (TES) integrated heat pump system for residential buildings was proposed to meet the building's thermal demand while shifting the electric demand. The system can provide distributed grid service for demand-side management (DSM) by (1) providing long-term high efficiency with a newly designed heat pump; and (2) shifting electric demand diurnally using an underground TES.

To realize DSM strategies with the new system, a well-fitted control strategy should be properly designed. Conventional thermostat control with heuristic rules (rule-based control, RBC) can make control decisions depending on the current measurement and pre-defined rules. The implementation for RBC is relatively simple. However, it is difficult for the RBC to integrate all useful information (e.g., forecasted load and weather) to fully explore the system's potential on approaching high thermal efficiency and flexibility. With decreasing costs in computation and sensing, advanced control strategies like model predictive control (MPC) have become popular research topics in building operations. Improving sensing and forecasting techniques on weather, occupancy, etc., enables accurate prediction of building thermodynamics using simplified mathematical models (Drgoňa et al., 2020). Given the fact that the thermal response time of the building is moderate, MPC is effective and suitable for building thermal system control on achieving optimal operation results. Specifically, with predictable grid conditions, the building thermal system with MPC can respond intelligently to realize DSM goals while satisfying the room thermal comfort requirement.

Unlike commercial buildings, MPC for residential thermal systems conducting various DSM is less studied. The most widely used indicator for DSM is operating cost reduction. Baniasadi et al. (2019) applied a time-of-use (TOU) tariff to a smart residential building in Australia that incorporated a heat pump, TES water tank, rooftop P.V., and battery to achieve minimum cost. The results indicated that a reduced daily energy cost could be as high as 44% in summer and 18% in winter. Golmohamadi et al. (2021) applied day-ahead pricing to minimize the operating cost in a residential building in Denmark by taking advantage of the building's thermal inertia and an active TES water tank. The results showed a weekly energy cost reduction of 37% in winter. Other indicators like the primary energy factor (a reflection of renewable power penetration) can also be used to evaluate DSM performance. Wolisz et al. (2020) developed an MPC to reduce the primary energy demand by activating the building thermal mass of a residential building in Germany. The result shows that the optimization control strategy successfully activated the building thermal mass, and the primary energy demand can be reduced by 3-7% annually. D'Ettorre et al. (2019) numerically studied the impact of integrating a stratified water tank with an air-source heat pump (ASHP) for space heating in Italy. With a proposed MPC for cost minimization, the results show that a water tank with 500 L volume would lead to an energy cost saving of up to 8% and a reduction of primary energy consumption by up to 13%, which is much higher than that in Wolisz et al. (2020). It indicates that TES tanks can provide more DSM flexibility than using the thermal mass of residential buildings.

Existing literature shows that MPC can exploit the TES integrated residential building thermal systems for DSM. However, most of the studies focus on heating scenarios. In addition, the stratified water tank is the dominant TES system used in the previous studies. It has low storage capacity and requires considerable installment space, demanding for residential buildings. Moreover, the MPC developed in many previous studies decoupled the building envelope model from the mechanical system and over-simplified the component models to neglect their nonlinearity for easier optimization problem-solving.

This paper presents an MPC for the novel TES integrated heat pump system for residential buildings to provide grid service for DSM in the cooling season. The MPC uses a simple dynamic model that couples the building envelope and the mechanical system. The modeled TES tank uses phase change material (PCM) to increase its energy storage density. A customized optimization solver is developed to account for the system's inherent nonlinearity. A case study is conducted to compare the performance of the system resulting from using the MPC and a typical RBC.

2. SYSTEM CONFIGURATION

The proposed system is targeted at single-family houses. The mechanical system mainly consists of a dual-source heat pump (DSHP) and a dual-purpose underground thermal battery (DPUTB), as depicted in Figure 1. The DSHP is an electricity-driven vapor compression heat pump that utilizes either the ambient air or the ground as its heat source/sink. It runs as an air-source heat pump (ASHP) when the ambient temperature is favorable and switches to a ground-source heat pump (GSHP) when the ambient air temperature is too high or too low. The source side of the GSHP connects to the helical heat exchanger submerged in the outer tank of the DPUTB. The heating/cooling load

from the helical heat exchanger will finally be rejected to the surrounding soil. At the room side, a fan coil works as the terminal that heats up or cools down the indoor air through forced convection. DPUTB is an innovative design that integrates TES into a shallow-buried ground heat exchanger (a detailed configuration of the DPUTB can be found in Shi et al., 2021). The tank is installed in the subsurface of the ground so that no TES installment space is needed in the room. The inner tank of the DPUTB works as a TES tank. Macro-encapsulated PCM is applied to enhance its storage capacity. PCM cans are installed layer by layer with limited space in between. The water flows through the gaps among PCM cans to freeze or melt PCMs. Proper flow direction is selected to maintain thermal stratification within the tank. The outer tank of the DPUTB works as a ground heat exchanger. A helical coil heat exchanger is installed in the outer tank that connects the DPUTB to the source side of the ground-source heat pump. The strong natural convection induced by the helical heat exchanger will keep the outer tank water well mixed. Therefore, the temperature of the helical coil leaving the water, in response to the heating/cooling input, is buffered by the entire water body in the outer tank.

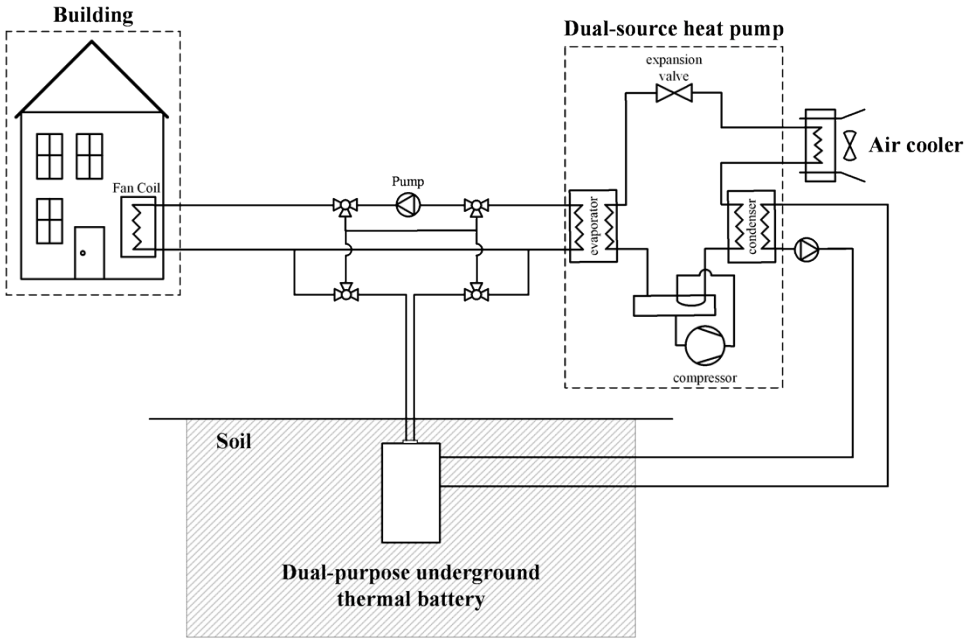

Figure 1: Schematic of a DPUTB integrated DSHP system for a single-family house

3. METHODOLOGY

3.1 Overview

MPC discretizes the prediction horizon in small sample times. Given future boundary conditions, it is capable of predicting building thermal response and guiding on control sequence so that an objective within the prediction horizon can be achieved. To implement MPC in an integrated building energy system, three key components are required: disturbance, model predictive controller, and a testbed. They are shown in Figure 2.

The disturbance is the non-controllable input of the MPC. Typically, the disturbances include weather conditions (e.g., ambient temperature, solar radiation, etc.), internal heat gains (e.g., occupancy, equipment, etc.), and grid information (e.g., electricity price). Model predictive controller development is the key component for the entire MPC scheme. A dynamic system model was developed to predict the thermal response of the building and the mechanical system. The model was simple enough so that it could be efficiently solved in the optimization problem. The cost function described the objective of the control: for the current study, minimizing the operating cost according to a TOU tariff. The output of the optimization problem was a sequence of 'future' control actions. Only the first control signal was sent to the mechanical system. With proceeding time, the prediction horizon kept being shift forward, and the optimization problem was always updated with new disturbances and states. In this way, the MPC was in a closed-loop, and this principle is called 'receding horizon control.' The testbed of the system can be either a real building energy system with measurement or a detailed building simulation model that incorporates many trustworthy sub-models. For the current study, the testbed is a simple simulation model similar to the dynamic

model in the model predictive controller. Typically, an estimator (e.g., Kalman Filter) is implemented to estimate those state variables that cannot be measured directly.

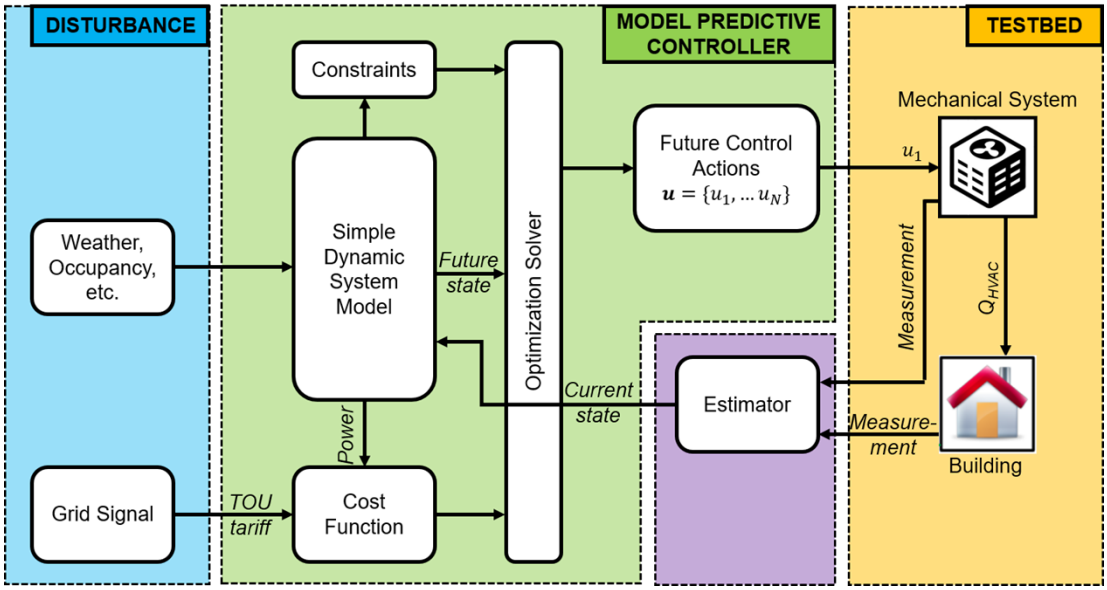

Figure 2: MPC scheme for the current study

3.2 Dynamic Model for MPC

As shown in Figure 1, to formulate our MPC controller, we need to develop dynamic models for building envelope, DSHP, and DPUTB, respectively.

3.2.1 Building envelope model. Gray-box models are widely used in model predictive control for building modeling due to their good balance of accuracy and computation speed. A typical representation of the gray-box model is the reduced-order Resistance-Capacitance (R.C.) model. Its accuracy is guaranteed by system identification from measured data or detailed building model simulation, and the computation speed can be enhanced since the number and complexity of differential equations are greatly reduced. The current study focuses on the model predictive control development of the mechanical system, but not the system identification of the R.C. model. Thus, the building model is further simplified as 0R1C with a given pre-calculated load. The model needs 1C to represent the lumped thermal capacitance of the building. The simplified building model can be expressed as:

$$C_{room}\frac{\mathrm{d}T_{room}}{\mathrm{d}t} = q_{load} + u_{FC}\cdot\left[u_{TES}\cdot mFR_{pump}\cdot c_p\cdot\left(T_{w1,in}-T_{w1,out}\right) - u_{GSHP}\cdot q_{GSHP} - u_{ASHP}\cdot q_{ASHP}\right] \quad (1)$$

3.2.2 DSHP model. For computational efficiency, a curve-fit method was adopted to simulate the DSHP. Catalog data from the heat pump manufacturers were used to generate the performance curves for the power and capacity prediction of the heat pump. Notice that the DSHP model is steady-state, and it is expressed in the algebraic equation instead of a first-order differential equation since it is fluid machinery with negligible stationary thermal mass. For the current study, a single-stage heat pump with constant flow rates on both load and source sides is applied. The heat pump performance is affected by the entering fluid temperatures at both the source and load sides. The performance can be expressed as below:

$$\dot{Q} = \left(\alpha_1 + \alpha_2\cdot\frac{T_{loa,ent}}{T_{loa,ref}} + \alpha_3\cdot\frac{T_{sou,ent}}{T_{sou,ref}}\right)\cdot\dot{Q}_{ref}\cdot s \quad (2)$$

$$P = \left(\beta_1 + \beta_2\cdot\frac{T_{loa,ent}}{T_{loa,ref}} + \beta_3\cdot\frac{T_{sou,ent}}{T_{sou,ref}}\right)\cdot P_{ref}\cdot s \quad (3)$$

3.2.3 DPUTB model. We have developed a detailed DPUTB model in a previous study (Shi et al., 2020), which can predict the thermal response of the DPUTB with good accuracy. However, it is too complex to be used in MPC. Instead, we use simple first-order differential equations to determine the required states.

The first important state is the in/outlet temperatures of the TES (inner tank of the DPUTB). Even though the inner tank is simulated as a stratified tank in the detailed model, to avoid listing numerous equations reflecting the temperature glide along the vertical direction, the inner tank water is simplified as a lumped control volume, and an average temperature of it is proposed to represent the inner tank water status. For the in/outlet temperatures, a constant temperature difference is assumed between the average temperature and the top/bottom parts of the inner tank. The first-order differential equation for the inner tank water can be expressed as:

$$m_{w1} \cdot c_p \frac{\mathrm{d}T_{w1,avg}}{\mathrm{d}t} = -u_{TES} \cdot mFR_{pump} \cdot c_p \cdot \left(T_{w1,in} - T_{w1,out}\right) - UA_{w1-PCM} \cdot \left(T_{w1,avg} - T_{PCM,avg}\right) - UA_{w1-w2} \cdot \left(T_{w1,avg} - T_{w2,avg}\right) \quad (4)$$

The second state that needs to be expressed is the status of the stored energy in the TES. Since most of the useful stored energy is in the form of latent heat in the PCM, the total PCM solid fraction is chosen as the indicating state. Currently, for simplification, the PCM is assumed to have a fixed melting point. All PCMs in the inner tank are assumed to be lumped and the dynamic change of the total average PCM solid fraction can be expressed as:

$$\frac{\mathrm{d}\lambda_{PCM,avg}}{\mathrm{d}t} = -\frac{1}{CAP} \cdot UA_{w1-PCM} \cdot \left(T_{w1,avg} - T_{PCM,avg}\right) \quad (5)$$

The last important state for the DPUTB is the returning temperature of the ground heat exchanger, which is the helical coil submerged in the outer tank water. Roughly, this temperature is only influenced by the outer tank water temperature, given the assumption that the helical coil heat exchanger has steady performance. For the current study, it is assumed that the helical coil has perfect heat transfer. That is, the outlet temperature of the helical coil is identical to the average outer tank water temperature. Thus, a first-order differential equation representing the outer tank water average temperature is adequate, which can be expressed as:

$$m_{w2} \cdot c_p \frac{\mathrm{d}T_{w2,avg}}{\mathrm{d}t} = UA_{w1-w2} \cdot \left(T_{w1,avg} - T_{w2,avg}\right) - UA_{w2-soil} \cdot \left(T_{w2,avg} - T_{soil}\right) + u_{GSHP} \cdot q_{coil-w2} \quad (6)$$

3.3 Optimization Problem Formulation for MPC

Based on the models developed above, we can formulate our optimization problem framework, which generally includes cost function, constraints, and system dynamics. The objective of the current study is to take advantage of the proposed system and the TOU tariff to minimize the operating cost over the prediction horizon while keeping the indoor air temperature within the pre-described range. The optimal control problem can be expressed as:

$$\min_{u_1,u_2,\ldots,u_{N-1}} \sum_{k=1}^{N-1} P_{DSHP,k} \cdot \Delta t \cdot Price_k \quad (7a)$$

subject to

$$x_{k+1} = f(x_k, u_k, d_k) \quad (7b)$$

$$x_{lb,k} \leq x_k \leq x_{ub,k} \quad (7c)$$

Equation 7b defines the simplified dynamic equations for the entire thermal system. As illustrated in section 3.2, the proposed system is small-scale (4 first-order differential equations) but includes nonlinearity. Its nonlinearity is two-fold: 1. The control actions of the components are discontinuous. Most of them are on/off or switch control instead of continuous modulating control; 2. There are non-linear terms in dynamic equations that mix control variables and state variables. These characteristics of the current optimization result in a problem similar to shortest path searching, which can be solved using the dynamic programming method. Compared with using a complex non-linear mixed-integer programming (NLMIP) solver, dynamic programming can easily handle the nonlinearity of the system with acceptable computation speed due to a small-scale system.

3.4 Rule-based Control Development

To testify that the proposed system with MPC has better performance, as a reference, an RBC is designed. This control strategy is developed based on sensing the following states before each sample time: 1. The period of pricing (i.e., on-peak or off-peak), which depends on the TOU tariff structure; 2. The status of TES (i.e., fully discharged during the on-peak period or fully charged during the off-peak period) depends on the working fluid temperature at the top/bottom of the DPUTB inner tank; 3. Thermal load requirement from fan coil (i.e., 0 or 1), which depends on

the room temperature or the set-point; 4. The selection of heat pump source (i.e., air-source or ground-source) depends on the ambient temperature.

4. CASE STUDY

A simulation-based case study was implemented to investigate the performance of the DPUTB integrated DSHP system under MPC and RBC strategies. A three-day simulation from July 25-27 was conducted for a single-family house located in Atlanta, GA. The prediction horizon and sample time choosing play a significant role in the performance of MPC. It is a trade-off between accuracy and computational speed. For the current study, the prediction horizon was chosen as 24 hours which always contains enough information for the next day's electricity price. The sample time was set as 15 minutes, considering the thermal response time of the building thermal mass and TES. For one-step optimization, it took the MATLAB-based dynamic programming solver 90 seconds to give optimal control outputs on a P.C. with Core i7-6700 CPU 3.41 GHz.

4.1 Testbed

The testbed of the control is either a real building with sensor measurement or a detailed simulation model that can predict the thermal response of the system. Currently, for simplicity, a simple model similar to the dynamic model in MPC was used. Equations 1-5 were applied for the simulation testbed to predict the dynamic change of room temperature, DPUTB inner tank water average temperature, PCM average charging status, and thermal output of the heat pump. For the borehole wall soil temperature, the g-function method was applied to predict its thermal response. Thus, the DPUTB outer tank water temperature was predicted by an energy balance, assuming it is in steady state at the end of each sample time.

The g-function is a non-dimensional temperature response factor proposed by Eskilson and Claesson (1988). Its value is determined by regression of the thermal response of detailed numerical or analytical borehole simulation. Given undisturbed soil temperature and the thermal input at each time step in history, the borehole wall soil temperature can be predicted using the following equation:

$$T_{soil}(t_n) = T_{ug} + \sum_{i=1}^{n} \frac{(Q_i - Q_{i-1})}{2\pi k} g(t_n - t_{i-1}) \tag{8}$$

The short-time g-function curve used in this study is a modified one from a UC Davis report (2021).

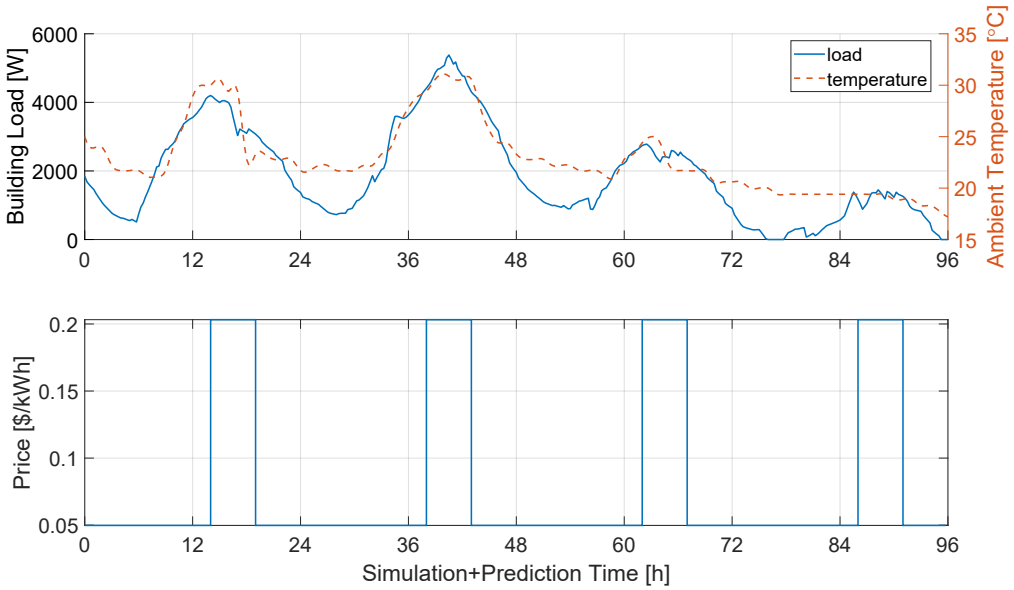

Figure 3: Disturbances for the case study, single-family house in Atlanta, July 25-28

4.2 Disturbances and Other Inputs

Hourly TMY3 data for Atlanta, GA, was used as the weather data. Given the weather condition, the hourly thermal load of a typical single-family house was determined with the EnergyPlus program using a prototype building model (DOE, 2021) in Atlanta, GA. The building load profile and ambient temperature profile from July 25-28 are shown in Figure 3.

A full-size DPUTB alone can provide the heat sink for a GSHP with 0.5-1 ton capacity. As a TES, its capacity is a combination of the PCM latent heat and the water sensible heat. The total volume of the PCM is 0.168 $m^{3,}$ and it occupies 18% of the inner tank volume. The volumetric energy density of the PCM used for simulation is 300 $MJ/m^{3,}$ and the total latent heat is 50.4 MJ, which is equivalent to 1-ton cooling for 4 hours. The melting point of the PCM is set as 9.5 °C. Because the maximum building thermal load is around 2 tons (from the annual building load profile), 2 full-size DPUTB would be needed. The thermal load of the building was divided by two to simplify the system simulation, and it is used to size the system. Thus only 1 DPUTB is included in the simulation. For half of the maximum building load, a heat pump with a 1-ton capacity at rated condition is large enough.

4.3 Results and Discussions

Thermal outputs of the proposed system operated with RBC and MPC, respectively, are plotted in Fig. 4 for a 3-day period. One clarification is that positive values for TES output indicate that TES is being discharged (i.e., releasing stored cooling energy), while negative values indicate it is being charged (i.e., storing cooling energy).

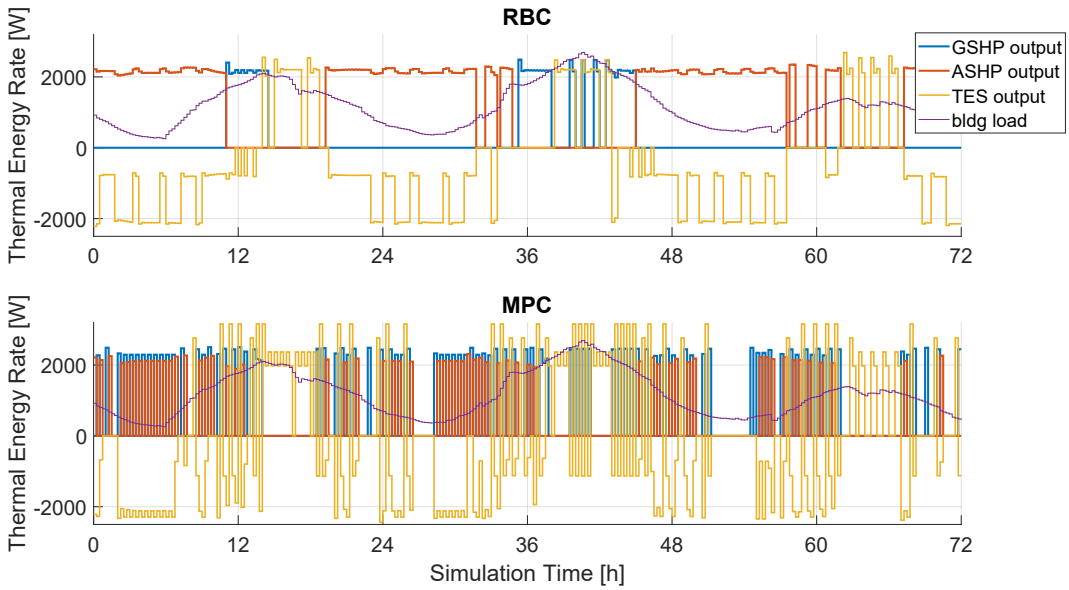

Figure 4: Thermal output profile

For RBC, the system always followed the pre-defined rule—during the off-peak period (0:00 to 14:00 and 19:00 to 24:00), the cooling demand of the building is always met soly by the heat pump, and the extra cooling output of the heat pump is used to charge the TES if it has not been fully charged; during the on-peak period (14:00 to 19:00), discharging TES takes high priority to satisfy the cooling demand unless it is fully discharged or the TES output rate is not enough to meet the cooling demand and maintain the room temperature within setpoints (21-23°C). The heat sink of the heat pump during cooling operation is selected based on a pre-defined ambient air temperature threshold, which is set to 26 °C. It can be observed that when the ambient air temperature is high (mid of the day for the first two days as shown in Figure 3), the ground source is used; otherwise, air-source is used.

For MPC, becasuse the objective is to minimize the operating cost, it results in more frequent swiches between air- and ground-source than RBC. It is to ensure the system is always running at a higher efficiency betweening using the available air- and ground-source. The system tries its best to avoid using any electricity during the peak period. Different from RBC, during the off-peak period, the system operated with MPC sometimes discharged TES for better cost-saving performance. This is a consequence of the system overall COP estimation according to predicted disturbances.

The intelligence of MPC is demonstrated in Figure 5, which shows the heat pump power consumption and the corresponding coefficient of performance (COP). It can be observed that the MPC frequently switches the heat pump source to keep the COP of the system as high as 3.5. However, for RBC, when the air source is used, the COP can be as low as 2.6. And a continuous using of GSHP would result in a lower COP according to g-function. Besides, Figure 5 indicates that the MPC turns on the heat pump less often than the RBC. It indicates another advantage of MPC—an intelligent TES charging strategy, which is illustrated in Figure 6.

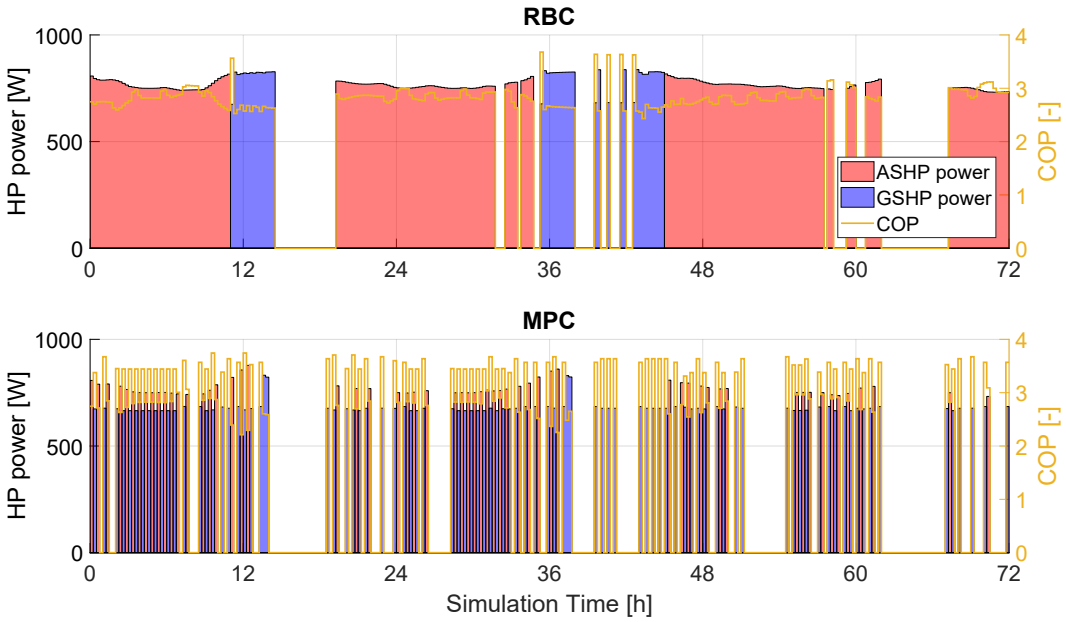

Figure 5: Heat pump power and COP profile

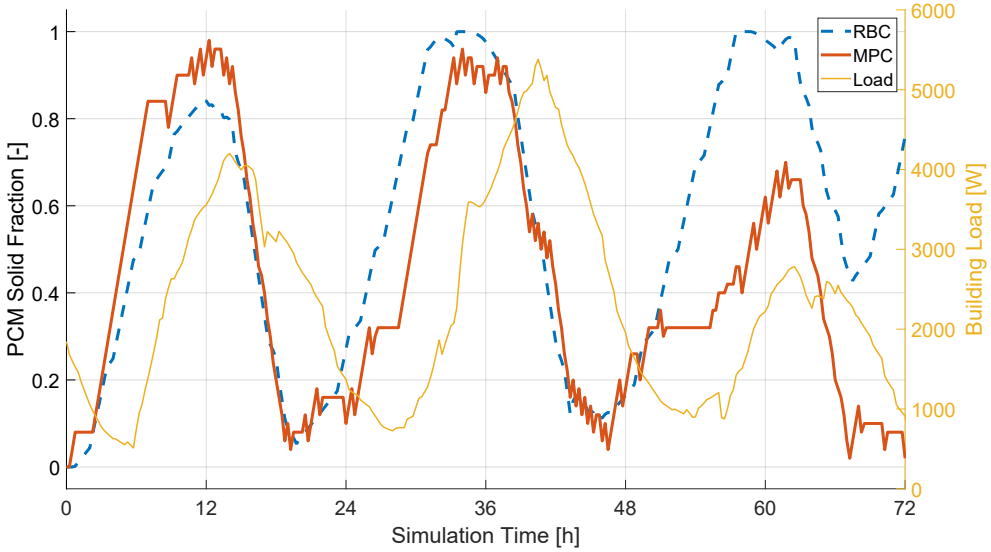

Figure 6: PCM total solid fraction profile

Figure 6 compares the PCM solid fraction profile resulting from the two control strategies. It can be observed that RBC always follows the pre-defined rule (i.e., charge the TES until it is full during the off-peak period). The TES is not fully charged for the first day because the TES is completely discharged at the begning and the charging time is limited. The disadvantage of a high charging ratio is that it leads to noticeable thermal loss to the outer tank, which results in a low overall thermal efficiency of the system. However, for the MPC, it can choose the charging level

according to the next day's on-peak period total cooling demand. It is noted that the third-day on-peak cooling demand is much less than the first two days, so the MPC only charges the TES to 70% before the on-peak period on the third day. This operation showed the advantage of MPC over RBC since it is capable of adjusting the charging operation based on the predited needs for stored cooling energy, which can reduce heat loss during standby and improve the overall efficiency of the integrated system during a given time period.

Table 2 summarizes the overall energy consumption and operation cost during the 3-day period. The MPC results savings in both the energy consumption and operating cost compared with the RBC. With minimizing cost as the objective, the MPC saves 38.5% operating cost and reduces 36.9% energy consumption compared with the RBC. It should be noted that the 3-day simulation period may be too short to reflect the real difference between the two controls. The cost reduction rate may not be as high as that in this 3-day period when the system is operated for a cooling season. However, the results during the 3-day period indicate that the MPC is more inteligent than RBC by taking advantages of the forecasted cooling demands and the performance of the integrated system.

Table 2: Summary of total energy consumption and operating cost during a 3-day perod

	Energy Consumption [kWh]	**Energy Reduction [%]**	**Operating Cost [$]**	**Cost Reduction [%]**
RBC	42.6	-	2.39	-
MPC	26.9	-36.9	1.47	-38.5

5. CONCLUSIONS AND FUTURE WORK

An MPC for a novel integrated TES and heat pump system for residential buildings has been developed and evaluated by comparing its performance with a typical RBC through a case study. Simulation results indicate that, operated with the MPC, the integrated TES and heat pump system meets the cooling demand of a typical single family home with high efficiency and shifts electric demand from on-peak to off-peak hours of the electric grid on a daily basis in response to a ToU electricity tariff.

The MPC is developed with a set of simplified component models and a customized Dynamic Programming solver. The MPC can find the optimal control sequence for operating the integrated heat pump and TES system at real time based on forecasts of the cooling demand of the building and the performance of the system. The MPC takes 1.5 min to find the optimal operation mode (e.g., charging or discharging TES, and slecing air- or ground-source for the DSHP) at every 15-min time step over a 24-hour period.

By taking advantage of predicted disturbances, the MPC performs more intelligently than the RBC by (1) adjusting TES charging based on the needed cooling energy during the on-peak period and (2) swiching between air- and ground-source to ensure the DSHP always run at a higher efficiency. A case study shows that, for a 3-day operation, the MPC saves 36.9% energy and reduces 38.5% operating cost compared with a typical RBC.

There are some limitations in the current work that will be solved in the future:

1. The current dynamic system model used in MPC did not consider the detailed building envelope, and the building thermal load was given as input. A resistance-capacitance (RC) model or a data-driven model will be used in the MPC to predict the thermal load of a given building.
2. The error of the disturbances (e.g., the predicted thermal loads) was not considered. A self-adaptive feature for the building model will be implemented to improve the accuracy of the predicted thermal load.
3. The error of the dynamic system model was not considered. The system model will be calibrated with experimental data of an integrated heat pump and TES system to improve its accuracy. In addition, an algorithm for estimating the error of the model prediction will be implemented in the MPC to fine-tune the model predictions in real-time.

NOMENCLATURE

C	capacitance	(J/°C)
CAP	latent capacity	(J)
c_p	specific heat	(J/kg/°C)

d	disturbance	(-)
k	thermal conductivity	(W/m/°C)
m	mass	(kg)
mFR	mass flow rate	(kg/s)
N	number	(-)
P	power	(W)
Q̇/Q/q	heat transfer rate	(W)
s	scaling factor	
T	temperature	(°C)
t	time	(s)
UA	overall heat transfer coefficient	(W/°C)
u	control variable	(-)
x	state variable	(-)
λ	solid fraction	(-)
Subscript		
avg	average	
ent	entering	
FC	fan coil	
i/k/n	time step number	
loa	heat pump load side	
ref	reference	
sou	heat pump source side	
ug	undisturbed ground	
w1	DPUTB inner tank water	
w2	DPUTB outer tank water	

REFERENCES

Baniasadi, A., Habibi, D., Al-Saedi, W., & Masoum, M. A. (2019). A Cost-effective Thermal and Electrical Energy Storage Management Strategy for Smart Buildings. In *2019 IEEE PES Innovative Smart Grid Technologies Europe (ISGT-Europe)* (pp. 1-5). IEEE.

D'Ettorre, F., De Rosa, M., Conti, P., Testi, D., & Finn, D. (2019). Mapping the energy flexibility potential of single buildings equipped with optimally-controlled heat pump, gas boilers and thermal storage. *Sustainable Cities and Society*, *50*, 101689.

DOE (U.S. Department of Energy). *Building Energy Codes Program: Residential Prototype Building Models*. Last modified October 7, 2020, accessed February 20, 2021.

Drgoňa, J., Arroyo, J., Figueroa, I. C., Blum, D., Arendt, K., Kim, D., Ollé, E.P., Oravec, J., Wetter, M., Vrabie, D.L., & Helsen, L. (2020). All you need to know about model predictive control for buildings. Annual Reviews in Control, 50, 190-232.

Eskilson, P., & Claesson, J. (1988). Simulation model for thermally interacting heat extraction boreholes. *Numerical heat transfer*, *13*(2), 149-165.

Golmohamadi, H., Larsen, K. G., Jensen, P. G., & Hasrat, I. R. (2021). Optimization of power-to-heat flexibility for residential buildings in response to day-ahead electricity price. *Energy and Buildings*, *232*, 110665.

Neukomm, M., Nubbe, V., & Fares, R. (2019). Grid-interactive efficient buildings technical report series: Overview of research challenges and gaps.

Schwartz, L., Wei, M., Morrow, W., Deason, J., Schiller, S.R., Leventis, G., Smith, S., Leow, W.L., Levin, T., Plotkin, S., & Zhou, Y. (2017). Electricity end uses, energy efficiency, and distributed energy resources baseline.

Shi, L., Liu, X., Qu, M., Zhang, M., & Wang, L. (2021). *Numerical Modeling and Parametric Study of a Dual Purpose Underground Thermal Battery* (No. ORNL/TM-2020/1796). Oak Ridge National Lab. (ORNL), Oak Ridge, TN (United States).

University of California, Davis, 2021. Low-Cost, Large-Diameter Shallow Ground Loops for Ground-Coupled Heat Pumps.

Wolisz, H., Kull, T. M., Müller, D., & Kurnitski, J. (2020). Self-learning model predictive control for dynamic activation of structural thermal mass in residential buildings. *Energy and Buildings*, *207*, 109542.